JOURNAL OF SOLID STATE CHEMISTRY 112, 176–181 (1994)

An EXAFS Investigation on Copper(I–II) Related Nasicon-Type Phosphates

E. Fargin, I. Bussereau, R. Olazcuaga, and G. Le Flem

Laboratoire de Chimie du Solide du CNRS, Université Bordeaux I, 351 cours de la Libération, 33405 Talence Cedex, France

and

C. Cartier and H. Dexpert

Laboratoire d'Utilisation du Rayonnement Electromagnétique (LURE), CNRS-CEA-MEN, Bâtiment 209 D, Université Paris-Sud, 91405 Orsay Cedex, France

Received May 14, 1993; in revised form October 4, 1993; accepted October 6, 1993

An extended X-ray absorption fine structure study at the copper *K*-edge of Nasicon-type phosphates with formulas $Cu^{I}M_2(PO_4)_3$ (M = Ti, Zr), $A_{1-x}Cu^{I}_xZr_2(PO_4)_3$ ($0 < x \leq 1$, A = Na; $x = 0.5$, A = H) and $Cu^{II}_{0.5}M_2(PO_4)_3$ (M = Ti, Zr) is reported. For $Cu^{I}Zr_2(PO_4)_3$, $H_{0.5}Cu^{I}_{0.5}Zr_2(PO_4)_3$, and $Na_{1-x}Cu^{I}_xZr_2(PO_4)_3$ ($0 < x \leq 1$) copper pairs have been evidenced (Cu^{I}–Cu^{I} = 2.40 Å) in the M_1 site of the Nasicon structure. In contrast, for the copper(II) phosphates, the Cu^{2+} ions are surrounded by four oxygen atoms at about 1.95 Å. Copper distribution in these various materials is discussed in relation to structural parameters.

INTRODUCTION

The structure of the Nasicon-type phosphates whose prototype is $NaZr_2(PO_4)_3$ consists of a three-dimensional network formed by PO_4 tetrahedra sharing corners with ZrO_6 octahedra (1). The site occupied by sodium is an elongated antiprism formed by triangular faces of two ZrO_6 octahedra along the **c** axis of the hexagonal cell (Fig. 1). This site is usually called M_1. The framework creates also a large tenfold coordinated site M_2. Every M_1 site is surrounded by six M_2 sharing common triangular faces.

Copper Nasicon-type phosphates have been investigated mainly in two different fields of the solid state chemistry. Cu(I) zirconium phosphates are the first examples of copper(I)-rich fluorescent insulators (2, 3). On the other hand, oxidation of the Cu(I) phosphates, e.g., $Cu^{I}Ti_2(PO_4)_3$ or $Cu^{I}Zr_2(PO_4)_3$, leads to the formation of Cu(II) phosphates with a reversible oxidoreduction process illustrated by the equation

$$4Cu^{I}M_2(PO_4)_3 + O_2 \rightleftarrows 4Cu^{II}_{0.5}M_2(PO_4)_3 + 2CuO.$$

Such a reaction, which does not alter the 3D framework, is at the origin of interesting catalytic behavior, e.g., the mild oxidation of propylene into acroleine and the oscillating activity in the decomposition of butanol (6, 7).

From a structural point of view in $Cu^{I}Ti_2(PO_4)_3$ and $Cu^{I}Zr_2(PO_4)_3$, the copper atoms are located in the M_1 site in an off-centered position giving rise to two short Cu–O distances: the copper surrounding is a compromise between the usual linear coordination and the geometry of the M_1 site. Copper pairs have been evidenced in $Cu^{I}Zr_2(PO_4)_3$ but not in $Cu^{I}Ti_2(PO_4)_3$ by a preliminary EXAFS investigation (9). The role of these clusters have been discussed with respect to the luminescent properties (3).

In contrast, the structures of the copper(II) phosphates are far from being completely understood. These materials could be prepared by solid state reaction(s) as well as via sol–gel routes (g) (10–12). Their unit cells exhibit different monoclinic distorsions which can be related to the hexagonal cell of the prototype.

Within these various contexts, the present paper reports a general EXAFS investigation of copper(I) and copper(II) Nasicon-type phosphates typical of situations resulting from the effects of the elaboration process of copper II phases, of the variation of copper(I) concentration and of the composition of the covalent framework (Zr vs Ti).

DATA COLLECTION

The X-ray absorption spectra of $A_{1-x}Cu^{I}_xZr_2(PO_4)_3$ (A = Na, x = 0.25, 0.5, 0.75; A = H, x = 0.5); $Cu^{I}M_2(PO_4)_3$, $Cu^{II}_{0.5}M_2(PO_4)_3$ (M = Ti, Zr) and the reference compounds Cu_2O and $Cu(CH_3COO)_2$ were recorded at LURE by using the EXAFS III spectrometer

0022-4596/94 $6.00

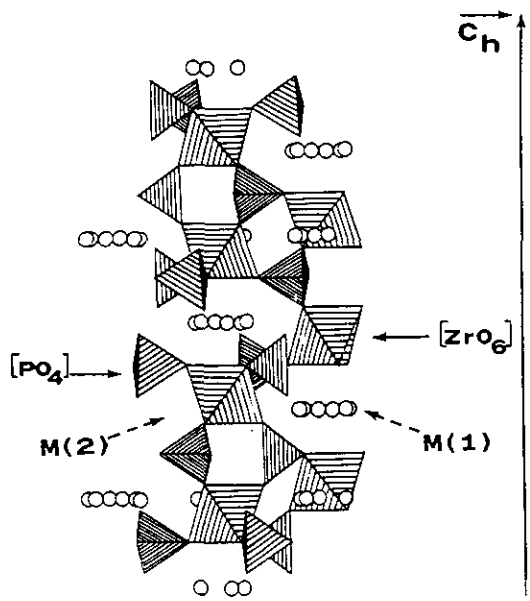

FIG. 1. The structure of $Cu^{I}Zr_2(PO_4)_3$.

in transmission mode at room temperature. This station is equipped with a two-crystal Si311 monochromator. During the experiment, the storage ring used 1.85-GeV positrons with an average intensity of 200 mA. Each material was powdered, uniformly dispersed, and sandwiched between two X-ray transparent Kapton adhesive tapes. Air filled ionization chambers were used to measure the flux intensity before and after the sample. Ten EXAFS spectra were then recorded for each sample within a 1000-eV range, with 2-eV steps and an accumulation time of 0.3 sec per point, and then averaged.

DATA ANALYSIS

The EXAFS analysis was carried out by using standard methods in the plane-wave approximation (13, 14). The continuous absorption background was estimated by fitting the spectrum before the edge by a linear function, while the main absorption beyond the edge $\mu(E)$ was fitted with an iterative procedure (13). The EXAFS contributions of the various shells are isolated by applying a k^3 weighted Fourier transform of $\chi(k)$ from k space to R space. The different peaks obtained in the resulting radial structure function correspond to individual coordination shells (Figs. 2 and 3).

The first peaks are separated between 1 and 1.9 Å and the second peaks between 1.9 and 2.8 Å for both copper(I) and copper(II) compounds. Each peak is back-transformed giving filtered EXAFS functions.

Then a least-squares fit of these filtered EXAFS signals, using phase shift and amplitude functions previously derived from the reference compounds, yields each shell atom identity and structural parameters N_j (average coordination number), R_j (average interatomic distance), and σ_j^2 (Debye–Waller factor). The accuracy of the fitted parameters has been estimated by treating one reference compound as an unknown using electronic parameters extracted from the other one. This procedure indicates errors of ±0.01 Å in R, ±20% in N for the first shell and ±0.02 Å in R, ±20% in N for the second shell. Second shell signals and least-squares simulations are given in Fig. 4.

RESULTS AND DISCUSSION

All the EXAFS simulation results are collected in Table 1.

A. The Copper(II) Phosphates

For all compounds, the first coordination shell is made up of four oxygen atoms at an average distance of 1.95 Å. The same result is also found for the amorphous material labeled g_{600} which is a gel of composition $Cu^{II}_{0.5}Zr_2(PO_4)_3$, dried at 600°C, i.e., just before the occuring of crystallization (12).

The intensity of the second shell peak in the Fourier transform is comparatively more important for the Zirconium phosphate (s) than for $Cu^{II}_{0.5}Ti_2(PO_4)_3$ which indi-

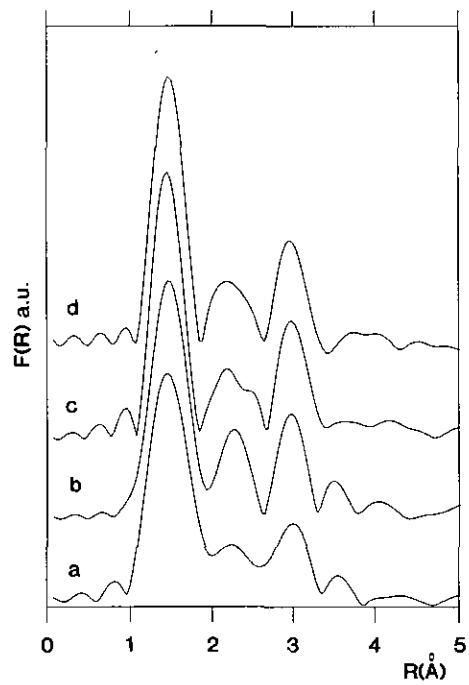

FIG. 2. Radial structure functions for Cu^{II} compounds: (a) $Cu^{II}_{0.5}Ti_2(PO_4)_3$, (b) $Cu^{II}_{0.5}Zr_2(PO_4)_3$ (s), (c) $Cu^{II}_{0.5}Zr_2(PO_4)_3$ (g_{600}), (d) $Cu^{II}_{0.5}Zr_2(PO_4)_3$ (g_{800}). (s), (g_{600}), and (g_{800}) indexes indicate that the materials have been prepared by a solid state route, a sol–gel route until 600°C, and a sol–gel route until 800°C respectively.

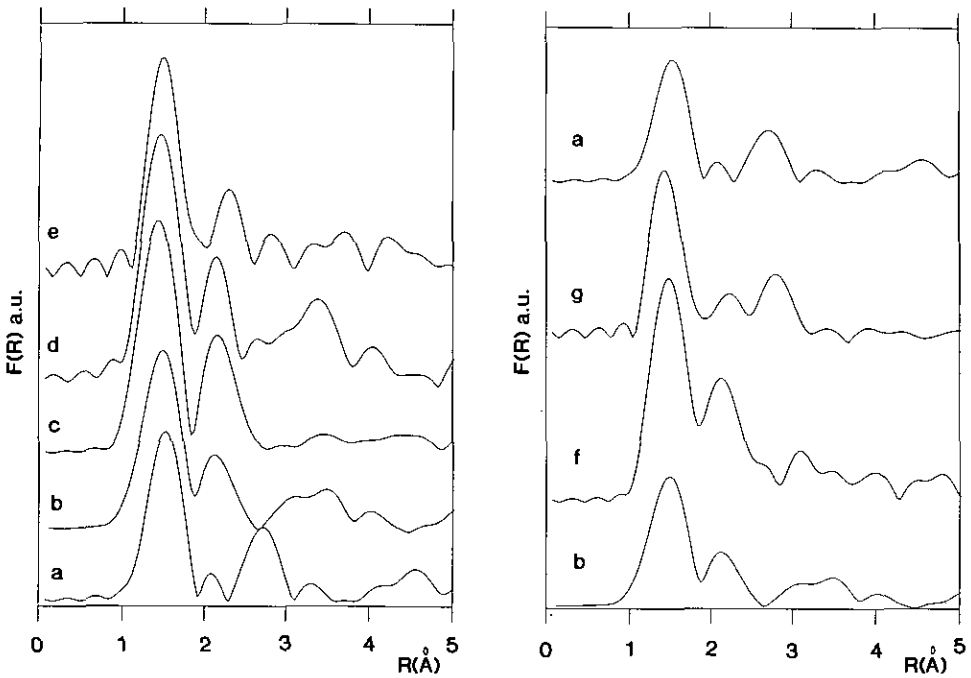

FIG. 3. Radial structure functions for Cu^{I} compounds: (a) $Cu^{I}Ti_2(PO_4)_3$ (b) $Cu^{I}Zr_2(PO_4)_3$, (c) $Na_{0.25}Cu^{I}_{0.75}Zr_2(PO_4)_3$, (d) $Na_{0.5}Cu^{I}_{0.5}Zr_2(PO_4)_3$, (e) $Na_{0.75}Cu^{I}_{0.25}Zr_2(PO_4)_3$, (f) $H_{0.5}Cu^{I}_{0.5}Zr_2(PO_4)_3$ (s), (g) $H_{0.5}Cu^{I}_{0.5}Zr_2(PO_4)_3$ (g). (s) and (g) indexes indicate that the materials have been prepared by a solid state and a sol–gel route, respectively.

cates the presence of heavy atoms as next nearest neighbors. Effectively the corresponding EXAFS signal can be closely fitted by introducing one copper atom at a distance of 2.76 Å and one oxygen atom at a distance of 2.81 Å. Thus half of the copper atoms are centered in M_1 sites whereas the others are located in the concomitant M_2 site and 75 ± 5% of M_1 sites remain consequently empty.

The EXAFS signals of the second shell for the two zirconium phosphates prepared by sol–gel routes (g_{600} and g_{800}) exhibit a beating at $k = 5$ Å^{-1} that is usually explained by the presence of one given atom at two different distances (Δd Cu–Cu = 0.3 Å) (15, 5). But in this case simulations using two different Cu–Cu distances have been attempted in vain.

Finally the third shell peaks in the Fourier transform which are attributed to zirconium atoms are similar for all the samples which is consistent with a preservation of the zirconium phosphate framework whatever the preparation conditions.

These results give a better insight into the crystal structure of these phases. At room temperature, $Cu^{II}_{0.5}Ti_2(PO_4)_3$ and $Cu^{II}_{0.5}Zr_2(PO_4)_3$ (s) are characterized by a rather large value of the c parameter of the equivalent hexagonal cell (10, 11). According to the rules governing the structural properties of the Nasicon-type phosphates, this behavior is correlated to the O^{2-}–O^{2-} repulsion occuring when a high proportion of M_1 is empty (16). In addition for $Cu^{II}_{0.5}Ti_2(PO_4)_3$, the absence of copper contribution to the second shell peak means that all the copper atoms are located in M_2. This conclusion is strongly in agreement with a recent structure determination of the high-temperature form (17).

The structure of the (g) form of $Cu^{II}_{0.5}Zr_2(PO_4)_3$ is rather of the $Sc_2(WO_4)_3$ type which has extensively been reported for $Ni_{0.5}Zr_2(PO_4)_3$ (18). The divalent ions are located in a strong distorted tetrahedron sharing two opposite edges with ZrO_6 octahedra. In this case the copper environment preexists in the amorphous phase (g_{600}).

B. The Copper(I) Phosphates

Figure 3 shows the radial structure functions for $Cu^{I}M_2(PO_4)_3$ (M = Ti, Zr), $Na_{1-x}Cu^{I}_xZr_2(PO_4)_3$ and the hydrogenated compound $H_{0.5}Cu^{I}_{0.5}Zr_2(PO_4)_3$ (g and s forms).

Two oxygen atoms are found in the first coordination shell as it is usually observed for Cu^{I} oxides. The Cu–O distances (≈2 Å) are slightly less than those reported from X-ray or neutron diffraction investigations: 2.08 Å (X-ray) and 2.06 Å (neutron) for $Cu^{I}Ti_2(PO_4)_3$, 2.05 Å (X-ray) and 2.09 Å (neutron) for $Cu^{I}Zr_2(PO_4)_3$ (4, 8, 19). The second shell of $Cu^{I}Zr_2(PO_4)_3$ is partially constituted of copper atoms at a short distance: 2.40 Å. The EXAFS simulation of the studied samples gave an average number of copper pairs equal to 0.4. Since the number of M_1 sites is equal to the number of copper atoms 20 ± 6% of these

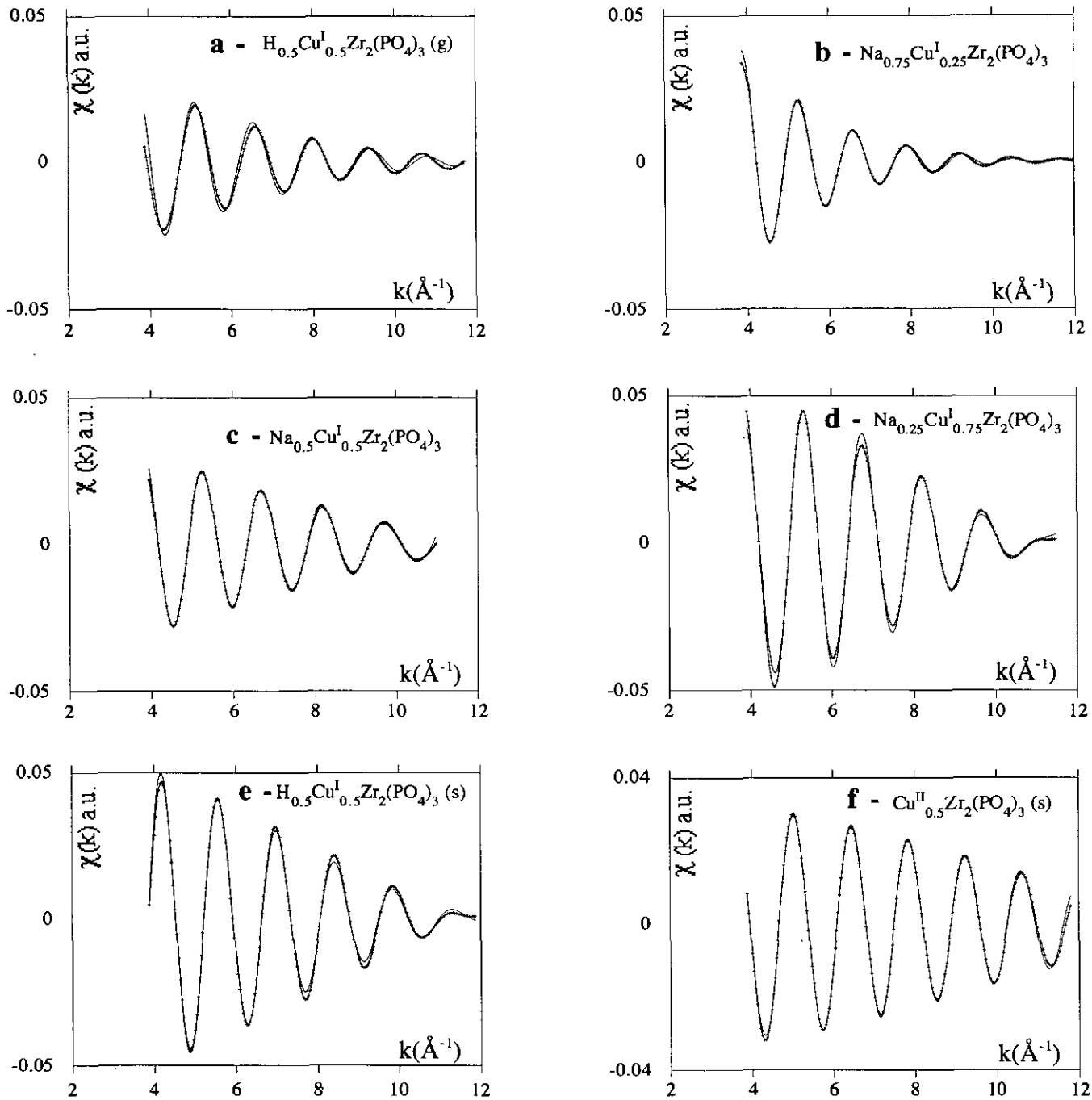

FIG. 4. EXAFS second shell signals (solid lines) and least-squares simulations (crossed lines) illustrating the absence (a, b) and the presence (c, d, e, f) of copper atoms in the second shell.

sites contain these pairs, 20 ± 6% remain empty whereas 60 ± 6% contain only one copper atom. In contrast for $Cu^{I}Ti_2(PO_4)_3$ the smaller size of M_1 site prevents the formation of such an association.

The same type of copper environment is observed for the solid solution $Na_{1-x}Cu^{I}_xZr_2(PO_4)_3$ (5). The two oxygen nearest neighbors are located at 1.99 ± 0.03 Å and the next ones at 2.81 Å for $x = 0.25$ and 2.72 Å for $x = 0.5$, 0.75, 1. With respect to the structure of $Cu^{I}Zr_2(PO_4)_3$ these last distances reflect the location of two oxygen respectively at 2.66 and 2.74 Å.

Copper (I) pairs are detected in the region $0 < x \leq 1$. In these aggregates, the Cu^{I}–Cu^{I} distances are remarkably constant 2.40 Å. The evolution of the number of pairs N

TABLE 1
Fitting Results for the EXAFS Spectra of Copper(I, II) Nasicon-Type Phosphates

Samples	Shell	R (Å)	N	$\Delta\sigma^2$ (Å^2)	E_0 (eV)
Cu^I					
$Cu^ITi_2(PO_4)_3$	Cu–O1	2.00	1.70	0.0039	8987.0
$Cu^IZr_2(PO_4)_3$	Cu–O1	1.99	2.00	0.0001	8996.4
	Cu–O2	2.73	1.63	0.0056	8995.5
	Cu–Cu	2.40	0.40	0.0039	9003.3
$Na_{0.25}Cu^I_{0.75}Zr_2(PO_4)_3$	Cu–O1	1.97	2.00	0.0011	8992.2
	Cu–O2	2.71	2.38	0.0011	8990.7
	Cu–Cu	2.40	0.80	0.0039	9004.4
$Na_{0.5}Cu^I_{0.5}Zr_2(PO_4)_3$	Cu–O1	1.96	2.00	0.0011	8991.8
	Cu–O2	2.72	1.65	0.0056	8990.9
	Cu–Cu	2.41	0.40	0.0011	9002.5
$Na_{0.75}Cu^I_{0.25}Zr_2(PO_4)_3$	Cu–O1	2.02	2.00	0.0056	8993.8
	Cu–O2	2.81	2.04	0.0075	8996.4
$H_{0.5}Cu^I_{0.5}Zr_2(PO_4)_3$ (g)	Cu–O1	1.97	2.00	0.0011	8993.4
	Cu–O2	2.72	2.00	0.0024	8997.3
$H_{0.5}Cu^I_{0.5}Zr_2(PO_4)_3$ (s)	Cu–O1	1.96	2.00	0.0024	8989.0
	Cu–O2	2.69	2.00	0.0011	8986.7
	Cu–Cu	2.39	0.80	0.0056	8998.0
Cu^{II}					
$Cu^{II}_{0.5}Ti_2(PO_4)_3$	Cu–O1	1.95	4.00	0.0011	8992.9
$Cu^{II}_{0.5}Zr_2(PO_4)_3$ (s)	Cu–O1	1.95	4.00	0.0011	8993.2
	Cu–O2	2.82	0.70	0.0001	8994.9
	Cu–Cu	2.76	0.92	0.0001	8976.9
$Cu^{II}_{0.5}Zr_2(PO_4)_3$ (g_{800})	Cu–O1	1.94	4.00	0.0024	8992.3
$Cu^{II}_{0.5}Zr_2(PO_4)_3$ (g_{600})	Cu–O1	1.94	4.00	0.0039	8992.7

Note. R (Å) (average interatomic distance), N (average coordination number), $\Delta\sigma$(Å^2) (Debye–Waller factor), E_0 (eV) (threshold energy).

is less precise. Within the accuracy of the estimation, their proportion tends to increase with x: undetected for $x = 0.25$; $10 \pm 3\%$ for $x = 0.5$; $30 \pm 9\%$ for $x = 0.75$; $20 \pm 6\%$ for $x = 1$.

The compounds $H_{0.5}Cu^I_{0.5}Zr_2(PO_4)_3$ are prepared by hydrogenation of the two phases $Cu^{II}_{0.5}Zr_2(PO_4)_3$ (g or s) according to the reaction

$$4Cu^{II}_{0.5}Zr_2(PO_4)_3 + H_2 \rightarrow 4H_{0.5}Cu^I_{0.5}Zr_2(PO_4)_3.$$

Two varieties can be obtained depending on the elaboration process of the starting materials (12, 20). They exhibit a monoclinic symmetry whose parameters of the equivalent hexagonal cell are respectively

(s) form $a = 8.84$ Å $c = 22.31$ Å
(g) form $a = 8.84$ Å $c = 21.35$ Å.

The first shell of copper in these two phases is also composed of two oxygens at 1.96 Å. The next nearest oxygen neighbors are found at 2.70 Å. The copper pairs (Cu^I–Cu^I = 2.39 Å) are detected only in the (s) form whose volume of the unit cell is larger. In this case, the proportion of doubly occupied M_1 sites is equal to $20 \pm 6\%$.

CONCLUSIONS

Whether the phosphates of Cu^I or Cu^{II} are concerned, the EXAFS results are in agreement with the structural features of the material already reported. As a general trend the calculated copper–oxygen distances are slightly lower than those deduced from X-ray or neutron diffraction studies.

Cu^+–Cu^+ pairs with a remarkably short and constant distance have been unambiguously evidenced. These pairs are at the origin of an intense yellow green luminescence observed for $Cu^IZr_2(PO_4)_3$ (2, 3) and related compounds, but more generally in materials containing large sites allowing copper aggregation: β'' alumina (21), zeolithe (22), etc. Such a pairing was predicted by means of molecular orbital calculation: a weak attractive interaction exists as a result of a mixing of 4*s* and 4*p* orbitals with 3*d* orbitals (23). They have been clearly reported in one organic sulfide $Cu_{2x}Cr_xSn_{2-2x}S_4$ and mostly in various organic complexes (24, 25).

REFERENCES

1. L. O. Hagman and P. Kierkegaard, *Acta Chem. Scand.* **22,** 1822 (1968).
2. G. Le Polles, C. Parent, R. Olazcuaga, and G. Le Flem, *C.R. Acad. Sci. Sér. II* **306,** 765 (1968).
3. P. Boutinaud, C. Parent, G. Le Flem, C. Pedrini, and B. Moine, *J. Phys. Condens. Matter* **4,** 3031 (1992).
4. M. Bandza, E. Bordes, P. Courtine, A. El Jazouli, J. L. Soubeyroux, G. Le Flem, and P. Hagenmuller, *React. Solids* **5,** 315 (1988).
5. I. Bussereau, Thesis, University of Bordeaux I, 1990.
6. L. Monceaux and P. Courtine, *Eur. J. Solid State Inorg. Chem.* **28,** 233 (1991).
7. A. Serghini, M. Kacimi, M. Ziyad, and R. Brochu, *J. Chim. Phys.* **85,** (4), 499 (1988).
8. I. Bussereau, M. S. Belkhiria, P. Gravereau, A. Boireau, J. L. Soubeyroux, R. Olazcuaga, and G. Le Flem, *Acta Crystallogr. Sect. C* **48,** 1741 (1992).
9. E. Fargin, I. Bussereau, G. Le Flem, R. Olazcuaga, C. Cartier, and H. Dexpert, *Eur. J. Solid State Inorg. Chem.* **29,** 975 (1992).
10. A. El Jazouli, J. L. Soubeyroux, J. M. Dance, and G. Le Flem, *J. Solid State Chem.* **65,** 351 (1986).
11. A. El Jazouli, M. Alami, R. Brochu, J. M. Dance, G. Le Flem, and P. Hagenmuller, *J. Solid State Chem.* **71,** 444 (1989).
12. I. Bussereau, R. Olazcuaga, G. Le Flem, and P. Hagenmuller, *Eur. J. Solid State Inorg. Chem.* **26,** 383 (1989).
13. B. K. Teo, "EXAFS: Basic Principles and Data Analysis," Springer Verlag, Berlin 1986.
14. We used the EXAFS Data Analysis set of programs written by A. Michalowicz, Ecole du CNRS "Structures Fines d'Absorption X en Chimie" (H. Dexpert, A. Michalowicz, and M. Verdaguer, Eds.), Vol. 3. Gardry, Sept. 1988.
15. A. Michalowicz, Thesis University of Paris Val de Marne, 1990.

16. F. Cherkaoui, J. C. Viala, C, Delmas, and P. Hagenmuller, *Solid State Ionics* **21,** p. 333 (1986).
17. A. Boireau, Thesis University of Bordeaux I, 1991.
18. A. Jouanneaux, A. Verbaere, Y. Piffard, A. M. Fitch, and M. Kinoshita, *Eur. J. Solid State Inorg. Chem.* **28,** 683 (1991).
19. E. M. McCarron, J. C. Calabrese, and M. B. Subramanian, *Mat. Res. Bull.* **22,** 1421 (1987).
20. G. Le Polles, A. El Jazouli, R. Olazcuaga, J. M. Dance, G. Le Flem, and P. Hagenmuller, *Mat. Res. Bull.* **22,** 1171 (1987).
21. J. D. Barrie, B. Dunn, G. Hollingsworth, and J. I. Zhink, *J. Phys. Chem.* **93,** 3958 (1989).
22. J. Texter, D. H. Strovie, R. G. Herman, and K. Keller, *J. Phys. Chem.* **81,** 333 (1977).
23. P. K. Mehotra and R. Hoffmann, *Inorg. Chem.* **17,** 2187 (1978).
24. S. Benazeth, M. Danot, P. Colombet, H. Dexpert, and P. Lagarde, *J. Phys. Colloq.* **47,** 777 (1986).
25. N. P. Rath, E. Holt and K. Tanibura, Inorg. Chem., **24,** p. 3934 (1985).